ISBN: 978-3-95450-247-9 ISSN: 2673-5490 doi: 10.18429/JACoW-IPAC2024-WEPG91

DESIGN OF AN ION-ACOUSTIC PROOF-OF-PRINCIPLE EXPERIMENT FOR LhARA*

M. Maxouti†[1,2,3], P.R. Hobson[4], B. Cox[5],
O. Jeremy[1], R.A. Amos[5], C. Whyte[6], J.C. Bamber[7], K. Long[1,2,3]
[1] Department of Physics, Imperial College London, UK
[2] John Adams Institute for Accelerator Science, UK
[3] Particle Physics Department, STFC Rutherford Appleton Laboratory, UK
[4] School of Physical and Chemical Sciences, Queen Mary University of London, UK
[5] Department of Medical Physics and Biomedical Engineering, University College London, UK
[6] Department of Physics, University of Strathclyde, UK
[7] Institute of Cancer Research and Royal Marsden NHS Foundation Trust, UK

Abstract

LhARA, the Laser-hybrid Accelerator for Radiobiological Applications, is a proposed facility for radiation biology research using ion beams. The accelerator is designed to deliver a variety of ion species at ultra-high dose rates and hence the delivered dose distribution should be measured in real-time to minimize uncertainties. A proof-of-principle experiment is presented that exploits the ultrasound waves induced from the absorption of the ion beam energy and the scintillation light emitted from a liquid scintillator. The proposed system has been evaluated in a series of Monte Carlo simulations using a 20 MeV proton beam to obtain a calibrated 3D dose map.

INTRODUCTION

Ions are used in radiotherapy due to their ability to deposit a maximum dose at the end of their range, in a sharp peak called the "Bragg peak", compared to x-rays that deposit dose along the entire path [1]. This feature is advantageous as it minimizes the impact on the healthy cells surrounding the tumour.

When an ion beam passes through a medium, the beam's energy is absorbed and causes a transient rise in pressure which results in the emission of an acoustic (pressure) wave that propagates within it [2]. Components of such waves can be detected using ultrasound transducers whose bandwidth is within the frequency range of the acoustic signals produced. The data can be used to form reconstruction components of the dose distribution by using appropriate algorithms.

Similarly, when the beam travels through a scintillator, the absorbed energy causes the emission of scintillation light. The luminescence is directly proportional to the energy absorbed, and hence, an appropriate optical system, such as a CMOS camera, can be used to detect and reconstruct the light distribution [3]. If the light yield of the scintillator is known, a calibrated dose distribution can be obtained.

* This work is supported by the Science and Technology Facilities Council (STFC).
† m.maxouti21@imperial.ac.uk

LhARA is designed to deliver a high flux of ion beams [4]. To ensure precise delivery of the required dose, the location of the Bragg peak, and the three-dimensional dose distribution, should be carefully monitored. For this purpose, a system is proposed that exploits the acoustic and optical signals induced when a 20 MeV proton beam propagates through a liquid scintillator phantom.

Acoustic methods offer real-time monitoring of ion beam propagation in biological tissues, while optical methods enable precise dose reconstruction within controlled environments like a phantom. By validating acoustic measurements with optical techniques, the acoustic measurements can be employed later to explore unknown experimental conditions.

METHOD

A cuboid phantom, the SmartPhantom, has been designed to be used as the beam energy absorber and propagating medium. Three windows on three orthogonal sides have been incorporated into the design to mount transducer arrays for detecting acoustic waves. The choice of transducer has been made to maximize the acoustic signal detection while minimizing the signal-to-noise ratio. The recovery of the 3D dose distribution was evaluated using an iterative time-reversal reconstruction algorithm [5].

A commercially available organic liquid scintillator is used to form a scintillating solution with water, mixed in a 50-50% ratio, that fills the volume of the phantom. The choice of the liquid scintillator was made to ensure that it is soluble in water and has a similar density to it to minimize the effect on the acoustic signal. An optical system of CMOS cameras and achromatic doublet lenses is used to image the scintillation light from two perpendicular angles. The obtained images are processed to recover the 3D light distribution that would be used for the acoustic calibration.

A series of simulations have been developed to evaluate the proposed system. The phantom and energy depositions of the beam in the scintillating solution have been simulated in Geant4 [6], the acoustic wave generation and detection have been simulated k-Wave [7], and the optical system in Ansys Zemax OpticStudio [8]. A 30 ns pulsed elliptical

ISBN: 978-3-95450-247-9 ISSN: 2673-5490 doi: 10.18429/JACoW-IPAC2024-WEPG91

proton beam with a kinetic energy of 20 MeV, 7.5% energy spread and approximately 20 mm diameter was used to irradiate the simulated SmartPhantom.

SMARTPHANTOM

Design The Computer Aided Design (CAD) of the SmartPhantom is shown in Figure 1. The phantom features a 15 mm diameter air-filled entry window sealed with a 50 μm thick matt-black Kapton foil. The length of the window stops at around 4 mm from the centre of the chamber to ensure that the Bragg peak of the 20 MeV beam occurs in the middle of the SmartPhantom. The interior surface is anodised black to reduce optical reflections.

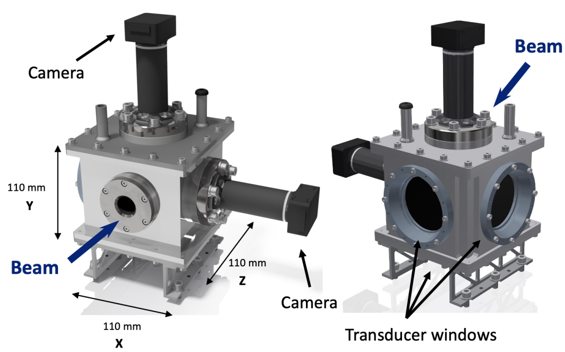

Figure 1: External view of the SmartPhantom. The design allows for simultaneous detection of the acoustic waves and scintillation light induced by the passage of ions.

Acoustic & Optical Windows Three acoustic windows have been designed. Two for mounting transducer arrays externally, coupled with a matt-black Kapton foil and an acoustic matching gel. A third window is used to immerse a single-element hydrophone to serve as a fixed reference for multiple experiment runs. To date, for the simulations, zero noise and infinite sensitivity have been assumed for all transducers. Two optical systems made of a pair of achromatic doublet lenses and CMOS cameras have been specified to capture, collimate and focus the scintillation light. The systems are placed perpendicularly to aid the reconstruction of the three-dimensional light distribution.

Geant4 Simulation The Geant4 simulation of the SmartPhantom is shown in Figure 2. Due to the complex mixture of organic molecules, the dominant compound in the chosen liquid scintillator has been used for the simulation. The energy depositions of the beam in the solution have been recorded in a three-dimensional matrix and used in the acoustic and optical simulations.

ACOUSTIC WAVE GENERATION & DETECTION

Pressure Distribution The pressure distribution is calculated using Equation (1), where $E(\mathbf{r},T)$ is the deposited energy distribution given by the Geant4 simulation and

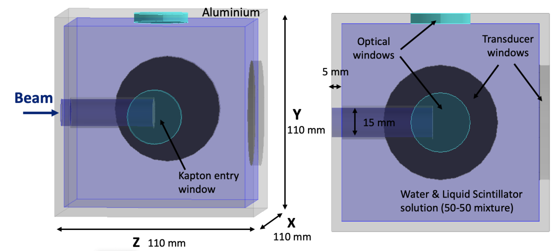

Figure 2: Geant4 simulation of the SmartPhantom.

$\Gamma(\mathbf{r},T)$ is the medium-dependent Grüneisen coefficient [9]. The calculated source pressure distribution is shown in Figure 3.

$$p_0(\mathbf{r},T) = \Gamma(\mathbf{r},T) \times E(\mathbf{r},T) \quad (1)$$

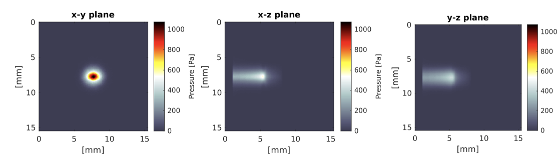

Figure 3: Calculated source pressure distribution based on the energy depositions given by the Geant4 simulation when a 20 MeV proton beam is absorbed in the SmartPhantom.

Acoustic Transducers Two transducer arrays are used to detect the acoustic waves; a matrix array of 32 by 32 square elements arranged in 4 banks and a linear array of 192 rectangular elements. The matrix array is placed on-axis with the beam to detect the location of the Bragg peak and the linear array is placed parallel to it to capture the axial shape of the Bragg curve and the radial profile of the proton beam. To detect the lower frequencies of the signal, a 13 mm diameter low-frequency single-element hydrophone is immersed in water and positioned 3 away from the Bragg peak. The transducers' positions relative to the proton beam depositions are shown in Figure 4.

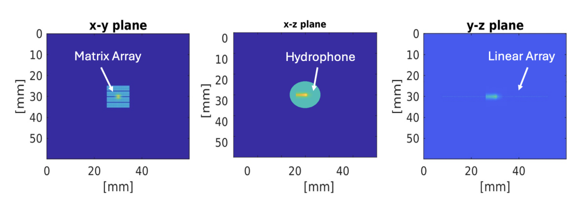

Figure 4: Matrix array transducer (left), single-element immersion hydrophone (middle) and linear array transducer (right) relative to the source pressure distribution caused by a 20 MeV proton beam travelling through the SmartPhantom.

LIQUID SCINTILLATOR

Ultima Gold XR The Ultima Gold XR cocktail was chosen to form a scintillating solution with water and fill the SmartPhantom's inner volume [10]. The cocktail's primary

ISBN: 978-3-95450-247-9 ISSN: 2673-5490 doi: 10.18429/JACoW-IPAC2024-WEPG91

compound is di-isopropyl naphthalene (DIPN). Measured refractive indices of Ultima Gold XR have been used for the optical simulation [11].

Zemax Simulation The energy depositions given by the Geant4 simulation have been used to predict the light intensity distribution. The optical sources are modelled as fifteen elliptical elements each emitting isotropically. The measured diffuse and specular reflection components from the matt-black Kapton windows and the anodized internal surface of the SmartPhantom at the scintillation peak emission wavelength of 427 nm have been used. In addition, non-sequential ray tracing has been used to enable the effects of specular and diffuse reflection, including polarization and realistic coatings on lenses. A side view of the simulated phantom and optical system is shown in Figure 5.

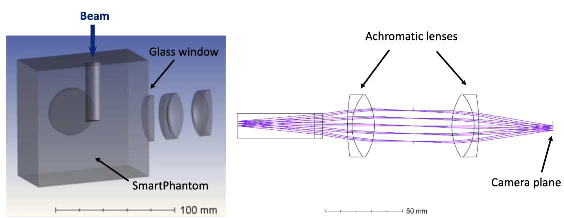

Figure 5: Zemax simulation of the SmartPhantom cut at the optical axis (left) and system of two identical lenses used for collimating and focusing the image onto the detector (right).

RESULTS & DISCUSSION

The acoustic reconstruction of the pressure distribution using the proposed transducers is shown in Figure 6. The reconstruction was performed using 4 iterations of an iterative

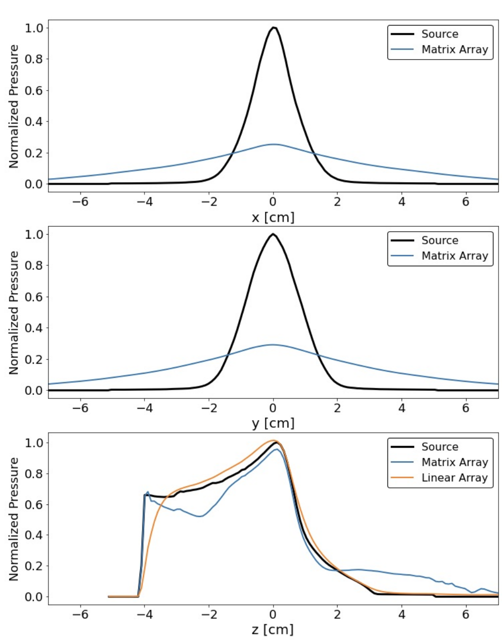

Figure 6: Reconstructed pressure distribution, in the three orthogonal axes, relative to the source pressure (black lines).

time-reversal algorithm. Four iterations of the algorithm have been considered sufficient for achieving convergence to the desired outcome.

The optical reconstruction of the scintillation light is shown in Figure 7. Figure 7 (left) shows the reconstructed image of the region in which the elliptical cylinder optical source is located. Figure 7 (right) shows the reconstructed irradiance through the central column (along the beam axis), normalized by area, to the relative Geant4 energy deposited by the proton beam in the scintillating solution.

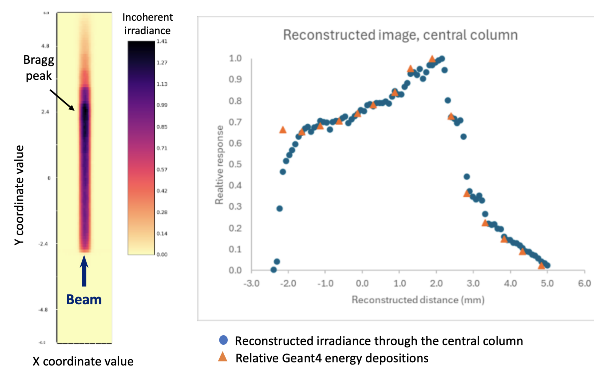

Figure 7: Reconstructed image irradiance on the camera plane (left) and reconstructed irradiance through the central column (right), binned in 50 μm $\times$ 100 μm pixels.

CONCLUSION

By combining the acoustic reconstructions using the proposed ultrasound transducers it is anticipated that a good impression of the three-dimensional pressure distribution caused by the ion beam's energy absorption in the SmartPhantom will be obtained. The Bragg peak, which is the dominant source of the acoustic waves, is well reconstructed using signals from the matrix array. The reconstruction of the radial profiles shows broadening due to its limited aperture. Improved reconstruction of the radial profile is expected from the linear array.

The optical simulation indicates that the proposed liquid scintillator and optics system can predict the three-dimensional energy deposition caused by the passage of the proton beam in the SmartPhantom.

In conclusion, the presented work indicates that a combination of the optical and acoustic systems can lead to a calibrated 3D dose map if the photon yield of the scintillating solution is known. Further development and validation of the ionacoustic approach would enable real-time 3D dosimetry during ion-beam radiation with LhARA.

ACKNOWLEDGEMENTS

This work was funded by the Science and Technology Facilities Council (STFC).

DATA AVAILABILITY

Data may be made available upon reasonable request.

ISBN: 978-3-95450-247-9 ISSN: 2673-5490 doi: 10.18429/JACoW-IPAC2024-WEPG91

REFERENCES

[1] E. J. Lehrer *et al.*, "Proton and Heavy Particle Intracranial Radiosurgery", *Biomedicines*, vol. 9, no. 1, p. 31, Jan. 2021. doi:10.3390/biomedicines9010031

[2] D. Haffa *et al.*, "I-BEAT: Ultrasonic method for online measurement of the energy distribution of a single ion bunch", *J. Manage. Sci. Rep.*, vol. 9, no. 1, p. 6714, Apr. 2019. doi:10.1038/s41598-019-42920-5

[3] D. Robertson, C. Hui, L. Archambault, R. Mohan, and S. Beddar, "Optical artefact characterization and correction in volumetric scintillation dosimetry", *Phys. Med. Biol.*, vol. 59, no. 1, pp. 23–42, Dec. 2013. doi:10.1088/0031-9155/59/1/23

[4] G. Aymar *et al.*, "LhARA: The Laser-hybrid Accelerator for Radiobiological Applications", *Front. Phys.*, vol. 8, p. 567738, Sep. 2020. doi:10.3389/fphy.2020.567738

[5] J. Otero, I. Felis, A. Herrero, J. A. Merchán, and M. Ardid, "Bragg Peak Localization with Piezoelectric *ACS Sens.* for Proton Therapy Treatment", *ACS Sens.*, vol. 20, no. 10, p. 2987, May 2020. doi:10.3390/s20102987

[6] Geant4, https://geant4.web.cern.ch

[7] k-Wave: A MATLAB toolbox for the time domain simulation of acoustic wave fields, http://www.k-wave.org

[8] Ansys Zemax OpticStudio, https://www.ansys.com/products/optics/ansys-zemax-opticstudio

[9] C. Freijo, J. L. Herraiz, D. Sanchez-Parcerisa, and J. M. Udias, "Dictionary-based protoacoustic dose map imaging for proton range verification", *Photoacoustics*, vol. 21, p. 100240, Mar. 2021. doi:10.1016/j.pacs.2021.100240

[10] Safety data sheet, https://resources.perkinelmer.com/corporate/content/msdsdatabase/msd_6013119_ultima_gold_xr_(gb).pdf

[11] K. Kossert, "Measurement of wavelength-dependent refractive indices of liquid scintillation cocktails", *Appl. Radiat. Isot.*, vol. 82, pp. 382–388, Dec. 2013. doi:10.1016/j.apradiso.2013.10.005